Project Report
Transportation of a Slung Load Using Multiple Quadrotors While Maintaining a Constant Altitude Above The Terrain

Tomer Levy
Advisor: Moshe Idan

March 23, 2020

Abstract

In this project the problem of carrying a single load using multiple quadrotors is being examined. The main goal is to build a control system that will enable us to transport the load safely while maintaining a constant altitude above the terrain. The report reviews the design of the simulation environment - the dynamic model of the quadrotors, load and the wires connecting between the load and the quadrotors. The report details a possible control structure for the above system. It combines a Linear Quadratic Regulator (LQR) controller that calculates required forces and moments such that the load will follow a certain trajectory. Then, an optimization problem is solved to divide the burden between the available quadrotors in an efficient way while fulfilling certain constraints. Finally, a geometric controller is developed such that each quadrotor will provide the required force. Simulation results testing the suggested control structure under different scenarios with and without disturbances are included. The work presented in this project provides the infrastructure for future research in the field of terrain following - specifically implementing a terrain following ability on a multi-UAV system.

1 Introduction

The subject of load transportation using a flock of unmanned aerial vehicles (UAVs) has been widely studied and developed in recent years, [1–4]. We will focus on using quadrotors as our UAVs, however, the theory and methods can be implemented for a large variety of multi-rotor platforms. Carrying a load using multiple small UAVs allows to significantly increase the maximum weight that can be carried using small quadrotors. Moreover, cooperation between multiple agents, although challenging, has many uses beside this project and thus is of great interest in the multi-rotor community.

In this project, modeling of the dynamics of a single quadrotor will be reviewed, followed by a model of a load attached to multiple quadrotors. Dynamic model of the wires will also be presented. Once we have a mathematical model for the system, a control structure that will allow the load to follow desired trajectory will be developed. At first, a Linear Quadratic Regulator (LQR) controller is designed to provide required forces and moments on the load center of gravity (c.g.) such that it will follow a certain trajectory. Then, an optimization problem is solved to divide the total forces and moments between the available quadrotors in some efficient way while maintaining certain constraints (quadrotor separation distance, maximum force for a single quadrotor, etc.). Finally, a geometric controller for a single quadrotor such that it will provide the required force is developed. Combining the above we get the full control structure for the system.

The first sections of the work explain the mathematical model developed for the simulation, Then, development of the above control structure is provided. The latter sections examine different simulation scenarios that test the controllers with and without disturbances. The last section will conclude with a summary of the work made in this project and a brief introduction to further research.

2 Mathematical model

In this section, mathematical equations that represent the quadrotors, load and cable dynamics will be reviewed and developed.

2.1 Dynamic model of the quadrotor

The dynamic model of the quadrotor was based on [5]. It should be noted that, in contrary to [5], the body frame of each quadrotor is set to be in a X configuration and not aligned with the rotors (see Fig. 1). The parameters of the quadrotor are given in Table 1. The equations of motion of the quadrotor

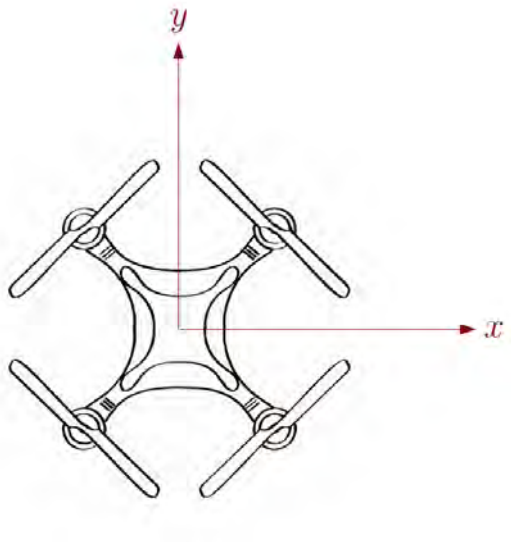

Figure 1: Quadrotor body frame coordinate system

are

$$\begin{Bmatrix} \ddot{x} \\ \ddot{y} \\ \ddot{z} \end{Bmatrix} = -\begin{Bmatrix} 0 \\ 0 \\ g \end{Bmatrix} - \frac{1}{m}\begin{bmatrix} A_x & 0 & 0 \\ 0 & A_y & 0 \\ 0 & 0 & A_z \end{bmatrix}\begin{Bmatrix} \dot{x} \\ \dot{y} \\ \dot{z} \end{Bmatrix} + \frac{1}{m}D_e^q \begin{Bmatrix} 0 \\ 0 \\ T \end{Bmatrix} \tag{1}$$

$$\begin{Bmatrix} \tau_\phi \\ \tau_\theta \\ \tau_\psi \end{Bmatrix} = I_q \begin{Bmatrix} \dot{p} \\ \dot{q} \\ \dot{r} \end{Bmatrix} + \begin{Bmatrix} p \\ q \\ r \end{Bmatrix} \times \left(I_q \begin{Bmatrix} p \\ q \\ r \end{Bmatrix} \right) \tag{2}$$

where

$$I_q = \begin{bmatrix} I_x & 0 & 0 \\ 0 & I_y & 0 \\ 0 & 0 & I_z \end{bmatrix}$$

is the tensor of moments of inertia of the quadrotor. D_e^q is the direction cosine matrix that transfer a body frame vector to inertial frame vector and defined as

$$D_e^q = \begin{bmatrix} cos\theta cos\psi & sin\phi sin\theta cos\psi - cos\phi sin\psi & cos\phi sin\theta cos\psi + sin\phi sin\psi \\ cos\theta sin\psi & sin\phi sin\theta sin\psi + cos\phi cos\psi & cos\phi sin\theta sin\psi - sin\phi cos\psi \\ -sin\theta & sin\phi cos\theta & cos\phi cos\theta \end{bmatrix}. \tag{3}$$

A_x, A_y, A_z are the drag coefficients linear in the quadrotor velocity. p, q, r are the body angular velocities. T is the thrust generated by the rotors and $\tau_\phi, \tau_\theta, \tau_\psi$ are the quadrotor moments around x, y and z accordingly. m is the quadrotor mass.

At this point, the only external forces that act on the quadrotor are the gravity force, drag and the thrust. It is assumed that the thrust and moments generated by the rotors are linear functions of the square of the rotor spin rates $\omega_i, i = 1, 2, 3, 4$ and are expressed as

$$\begin{Bmatrix} \tau_\phi & \tau_\theta & \tau_\psi & T \end{Bmatrix} = \begin{Bmatrix} \omega_1^2 & \omega_2^2 & \omega_3^2 & \omega_4^2 \end{Bmatrix} M_C^{-1}, \tag{4}$$

here, the matrix M_C stands for "Motor Coefficients" and represented as

$$M_C = \begin{bmatrix} \frac{1}{4kL\cos(45°)} & -\frac{1}{4kL\cos(45°)} & -\frac{1}{4kL\cos(45°)} & \frac{1}{4kL\cos(45°)} \\ -\frac{1}{4kL\cos(45°)} & -\frac{1}{4kL\cos(45°)} & \frac{1}{4kL\cos(45°)} & \frac{1}{4kL\cos(45°)} \\ -\frac{1}{4b} & \frac{1}{4b} & -\frac{1}{4b} & \frac{1}{4b} \\ \frac{1}{4k} & \frac{1}{4k} & \frac{1}{4k} & \frac{1}{4k} \end{bmatrix}$$

where k is the rotor lift constant, b is the rotor drag constant and L is the distance between a rotor and the quadrotor c.g.. Each motor dynamics was approximated as a first order transfer function

$$\frac{\omega}{\omega_{com}}(s) = \frac{1}{1+\tau s} \tag{5}$$

where τ represents the time constant of the motor. Once the load is added to the model, we insert the forces and moments applied by the cable connected to each quadrotor as external forces and moments and receive the following equations

$$\begin{Bmatrix} \ddot{x} \\ \ddot{y} \\ \ddot{z} \end{Bmatrix} = -\begin{Bmatrix} 0 \\ 0 \\ g \end{Bmatrix} - \frac{1}{m}\begin{bmatrix} A_x & 0 & 0 \\ 0 & A_y & 0 \\ 0 & 0 & A_z \end{bmatrix}\begin{Bmatrix} \dot{x} \\ \dot{y} \\ \dot{z} \end{Bmatrix} + \frac{1}{m}D_e^q\begin{Bmatrix} 0 \\ 0 \\ T \end{Bmatrix} - \frac{1}{m}\vec{F} \tag{6}$$

$$\begin{Bmatrix} \tau_\phi \\ \tau_\theta \\ \tau_\psi \end{Bmatrix} = I_q\begin{Bmatrix} \dot{p} \\ \dot{q} \\ \dot{r} \end{Bmatrix} + \begin{Bmatrix} p \\ q \\ r \end{Bmatrix} \times \left(I_q \begin{Bmatrix} p \\ q \\ r \end{Bmatrix} \right) + R_q \times \vec{F} \tag{7}$$

where $\vec{F}$ is the force that the cable applies on the load (opposite in sign to the force that the cable applies on the quadrotor). R_q is the vector connecting between the quadrotor c.g. and the cable attachment point on the quadrotor, given and fixed.

Table 1: Quadrotor parameters

Parameter	Value	Units	Interpretation
g	9.81	$\frac{m}{s^2}$	earth's gravity
m	0.468	kg	quadrotor mass
L	0.225	m	distance between a rotor and the quadrotor center of gravity
k	$2.98 \cdot 10^{-6}$	$kg \cdot m$	rotor lift constant
b	$1.14 \cdot 10^{-7}$	$kg \cdot m^2$	rotor drag constant
I_M	$3.357 \cdot 10^{-5}$	$kg \cdot m^2$	motor moment of inertia
I_x	$4.856 \cdot 10^{-3}$	$kg \cdot m^2$	quadrotor moment of inertia around x
I_y	$4.856 \cdot 10^{-3}$	$kg \cdot m^2$	quadrotor moment of inertia around y
I_z	$8.801 \cdot 10^{-3}$	$kg \cdot m^2$	quadrotor moment of inertia around z
A_x	0.25	$\frac{Ns}{m}$	quadrotor drag coefficient in the x direction
A_y	0.25	$\frac{Ns}{m}$	quadrotor drag coefficient in the y direction
A_z	0.25	$\frac{Ns}{m}$	quadrotor drag coefficient in the z direction
τ	0.01	sec	motor dynamics time constant

2.2 Dynamic model of the load

The load was modeled using the equations of motion, following the same principle as the modeling of the quadrotor, however, without control inputs (following the fact that the load has no propulsion mechanism). The load is affected only by external forces and moments - those that each quadrotor applies and the ones caused by gravity and drag. The load parameters are given in Table 2.

The load equations are

$$\begin{Bmatrix} \ddot{x} \\ \ddot{y} \\ \ddot{z} \end{Bmatrix} = -\begin{Bmatrix} 0 \\ 0 \\ g \end{Bmatrix} - \frac{1}{m_l}\begin{bmatrix} A_{lx} & 0 & 0 \\ 0 & A_{ly} & 0 \\ 0 & 0 & A_{lz} \end{bmatrix}\begin{Bmatrix} \dot{x} \\ \dot{y} \\ \dot{z} \end{Bmatrix} + \frac{1}{m_l}\sum_{i=1}^{n}\vec{F_i} \tag{8}$$

$$\begin{Bmatrix} \tau_\phi \\ \tau_\theta \\ \tau_\psi \end{Bmatrix} = I_l\begin{Bmatrix} \dot{p} \\ \dot{q} \\ \dot{r} \end{Bmatrix} + \begin{Bmatrix} p \\ q \\ r \end{Bmatrix} \times \left(I_l \begin{Bmatrix} p \\ q \\ r \end{Bmatrix} \right) - \sum_{i=1}^{n}\rho_i \times \vec{F_i} \tag{9}$$

where $\vec{F_i}$ is the force cable i applies on the load (which is, in other words, the force that quadrotor i applies). ρ_i, given and fixed, is the vector originating in the load c.g. and ends at the attachment point

between the i'th cable and the load. A_{lx}, A_{ly}, A_{lz} are the drag coefficients of the load and

$$I_l = \begin{bmatrix} I_{lx} & 0 & 0 \\ 0 & I_{ly} & 0 \\ 0 & 0 & I_{lz} \end{bmatrix}$$

is the tensor of moments of inertia of the load.

Table 2: Load and cable parameters

Parameter	Value	Units	Interpretation
m_l	0.4	kg	load mass
I_{lx}	0.0017	$kg \cdot m^2$	load moment of inertia around x
I_{ly}	0.0057	$kg \cdot m^2$	load moment of inertia around y
I_{lz}	0.0067	$kg \cdot m^2$	load moment of inertia around z
A_{lx}	0.3	$\frac{Ns}{m}$	load drag coefficient in the x direction
A_{ly}	0.3	$\frac{Ns}{m}$	load drag coefficient in the y direction
A_{lz}	0.3	$\frac{Ns}{m}$	load drag coefficient in the z direction
L_{load}	0.8	m	load length
W_{load}	0.4	m	load width
H_{load}	0.2	m	load height
ℓ	3	m	each cable length
K_s	100	$\frac{N}{m}$	cable spring constant
C_d	10	$\frac{kg}{s}$	cable damping constant

2.3 Wires model

Each wire connecting between each quadrotor to the load was modeled as a spring/damper system as shown in [1]

$$\vec{F_i} = F_{k,i} + F_{c,i}$$

where

$$F_{k,i} = \begin{cases} K_s \Delta\ell_i & \text{if } \Delta\ell_i > 0 \\ 0 & \text{if } \Delta\ell_i \leq 0 \end{cases} \tag{10}$$

and

$$F_{c,i} = \begin{cases} C_d \dot{\ell}_i & \text{if } \dot{\ell}_i > 0 \\ 0 & \text{if } \dot{\ell}_i \leq 0 \text{ or } \Delta\ell_i \leq 0 \end{cases} \tag{11}$$

where $\Delta\ell$ is the extension of the cable with respect to the nominal length ℓ. The values of K_s and C_d displayed in Table 2 were chosen in a way that the wires will be quite stiff, but not exaggerated due to numerical limitations.

3 Control design

This section discusses the design of the control structure for the system. During the work, many methods and attempts to find a proper control structure were made. The main approach was to divide the problem to three sub levels:

- On the top level we have a controller that calculates total required forces and moments such that the load will follow a desired trajectory. For that task, a LQR controller was chosen and designed. Other possible solution that was examined was to use Model Predictive Control (MPC). The advantage of the MPC is that it allows to calculate directly the desired forces that each quadrotor should provide such that it will fulfill certain constraints (minimum separation distance, maximum force for each quadrotor etc.). However, it was found to be more complex to properly design and limited in some aspects. Since the LQR does not include constraints, which is necessary to ensure feasibility of the solution, we move to the next level in the control structure.

- After receiving the total desired forces and moments, an optimization problem is solved to split those forces and moments between the different available quadrotors. The optimization takes under consideration relevant constraints. The solution provides the force that each quadrotor is required to apply.
- The final level is the flight controller for each quadrotor. Here, different controllers were designed and tested. At first, lead networks were designed. Those were proven to be stable and efficient to control a single quadrotor with no disturbances. However, once including a disturbance they were found to not be fast enough, hence, failed to fulfill the task. Next, PID controllers were tested and again did not provide satisfying results. Finally, a geometric controller based on [6] and [7] was designed and found to be fast and robust enough to fulfill the task. The prescribed geometric controller was adjusted to provide desired forces instead of following desired states.

3.1 Load desired forces and moments controller

Given desired trajectory we want the load to follow, we will use the LQR method to calculate a required set of forces and moments we need to apply on the load c.g. in order to follow that given trajectory. The initial guess for the LQR weights will be chosen using Bryson rule - the first weight of each control input or state is chosen to be one divided by the maximum acceptable error squared of that state or input. From there the weights were tuned by trial and error until sufficient results were achieved. The LQR gains were calculated for a simplified model which assumes the quadrotors provide immediately the required forces, and ignores the cable dynamics.

The simplified state space equations are:

$$\dot{x} = \begin{bmatrix} 0 & 0 & 0 & 0 & 0 & 0 & 1 & 0 & 0 & 0 & 0 & 0 \\ 0 & 0 & 0 & 0 & 0 & 0 & 0 & 1 & 0 & 0 & 0 & 0 \\ 0 & 0 & 0 & 0 & 0 & 0 & 0 & 0 & 1 & 0 & 0 & 0 \\ 0 & 0 & 0 & 0 & 0 & 0 & 0 & 0 & 0 & 1 & 0 & 0 \\ 0 & 0 & 0 & 0 & 0 & 0 & 0 & 0 & 0 & 0 & 1 & 0 \\ 0 & 0 & 0 & 0 & 0 & 0 & 0 & 0 & 0 & 0 & 0 & 1 \\ 0 & 0 & 0 & 0 & 0 & 0 & \frac{A_{lx}}{m_l} & 0 & 0 & 0 & 0 & 0 \\ 0 & 0 & 0 & 0 & 0 & 0 & 0 & \frac{A_{ly}}{m_l} & 0 & 0 & 0 & 0 \\ 0 & 0 & 0 & 0 & 0 & 0 & 0 & 0 & \frac{A_{lz}}{m_l} & 0 & 0 & 0 \\ 0 & 0 & 0 & 0 & 0 & 0 & 0 & 0 & 0 & 0 & 0 & 0 \\ 0 & 0 & 0 & 0 & 0 & 0 & 0 & 0 & 0 & 0 & 0 & 0 \\ 0 & 0 & 0 & 0 & 0 & 0 & 0 & 0 & 0 & 0 & 0 & 0 \end{bmatrix} x + \begin{bmatrix} 0 & 0 & 0 & 0 & 0 & 0 \\ 0 & 0 & 0 & 0 & 0 & 0 \\ 0 & 0 & 0 & 0 & 0 & 0 \\ 0 & 0 & 0 & 0 & 0 & 0 \\ 0 & 0 & 0 & 0 & 0 & 0 \\ 0 & 0 & 0 & 0 & 0 & 0 \\ \frac{1}{m_l} & 0 & 0 & 0 & 0 & 0 \\ 0 & \frac{1}{m_l} & 0 & 0 & 0 & 0 \\ 0 & 0 & \frac{1}{m_l} & 0 & 0 & 0 \\ 0 & 0 & 0 & \frac{1}{I_{lx}} & 0 & 0 \\ 0 & 0 & 0 & 0 & \frac{1}{I_{ly}} & 0 \\ 0 & 0 & 0 & 0 & 0 & \frac{1}{I_{lz}} \end{bmatrix} u \tag{12}$$

where

$$x = \begin{Bmatrix} x & y & z & \phi & \theta & \psi & \dot{x} & \dot{y} & \dot{z} & p & q & r \end{Bmatrix}^T \tag{13}$$

$$u = F_{CG} \tag{14}$$

and F_{CG} is the total required forces and moments applied on the load c.g. vector command:

$$F_{CG} = \begin{Bmatrix} F_x \\ F_y \\ F_z \\ M_x \\ M_y \\ M_z \end{Bmatrix}. \tag{15}$$

As a way to try and improve the performance and robustness against disturbances of the controller, an attempt to include integrators of the state errors and augment them to the LQR was conducted. Indeed, it was found to provide better results and to eliminate steady state errors caused by constant disturbances. The augmentation was conducted by summing the command of each control input as:

$$u_i = K_{i,LQR}\left(x_i, des - x_i\right) + K_{i,I}\int_0^t \left(x_i, des - x_i\right) d\tau \tag{16}$$

where the initial conditions were chosen to be zero and the augmentation was implemented over the position states only. A more accurate way to apply that augmentation would be to include the integrated error states in the state space realization and provide them with a relevant weight, then recalculate the LQR gains. This is left for future work, for our project, we will settle for the prescribed implementation. The calculated LQR gains for the simplified model was implemented to the full model and tested under numerical simulations, the chosen gains and weights will be displayed in the simulation section.

3.2 Optimization and constraints

Provided with the desired total forces and moments (F_{CG}), we now want to divide the burden in some efficient way between our set of quadrotors under certain constraints. To do that, we will define and solve the constrained optimization problem as described in [8]. We can present the moments and forces each quadrotor applies on the load c.g. as

$$F_{CG,i} = \begin{Bmatrix} \vec{F}_i \\ \rho_i \times \vec{F}_i \end{Bmatrix} = G_i \vec{F}_i, \tag{17}$$

as stated before, $\vec{F}_i$ is the force cable i applies on the load. G_i is the geometry matrix of each quadrotor defined as

$$G_i = \begin{bmatrix} 1 & 0 & 0 \\ 0 & 1 & 0 \\ 0 & 0 & 1 \\ 0 & -\rho_{i,z} & \rho_{i,y} \\ \rho_{i,z} & 0 & -\rho_{i,x} \\ -\rho_{i,y} & \rho_{i,x} & 0 \end{bmatrix}. \tag{18}$$

Here, $\rho_{i,j}$ are the components constructing the attachment point vector on the load i'th connection point, $\rho_i = \begin{Bmatrix} \rho_{i,x} & \rho_{i,y} & \rho_{i,z} \end{Bmatrix}^T$. The total forces and moments applied by the quadrotors on the load c.g. are given by

$$F_{CG} = G\vec{F} = \begin{Bmatrix} G_1 & G_2 & \cdots & G_n \end{Bmatrix} \begin{Bmatrix} \vec{F}_1 \\ \vec{F}_2 \\ \vdots \\ \vec{F}_n \end{Bmatrix}. \tag{19}$$

As mentioned before, for a given trajectory the desired F_{CG} (total forces and moments) is known. The goal is to find F_i for $i = 1, 2..., n$ in an effective way that will split the burden of the load among the quadrotors.

We will use the least norm solution defined as

$$F_{LN} = G^T \left(GG^T\right)^{-1} F_{CG}. \tag{20}$$

However, we still want to apply constraints on the quadrotors. In order to include those constraints we will use the null space of G which will be marked as G_{Null} and the final desired forces each quadrotor need to provide will be calculated as

$$\vec{F} = F_{LN} + G_{Null} c_r. \tag{21}$$

Here, c_r will be the optimization parameter and will be calculated by solving the optimization problem:

$$\min_{c_r} \quad \|F_{LN} + G_{Null} c_r\| \tag{22a}$$

$$\text{subject to} \quad \vec{h}\left(\vec{F}\right) \leq 0, \tag{22b}$$

where (22b) express the various constraints on the optimization problem. Different constraints can be considered such as:

- Safety distance between every two quadrotors.
- Keeping the cables taut at all times.

- Maximum allowed force each quadrotor can provide.
- The pointing direction of each force is limited to a certain region relative to the load surface (to prevent entanglement of the wires).

Constraints can be changed depending on usage and limitations of the system. Note that too strict constraints may end up in no possible solution, therefore, one must be careful and aware of the system limitations. The optimization problem was solved every discrete fixed time step using Matlab's "fmincon" function.

3.3 Geometric controller for the quadrotors

Given the desired forces each quadrotor is required to provide, we will use the geometric controller developed in [6, 7] with a few adjustments. The desired force each quadrotor should provide will be defined as

$$F_{des,i} = \vec{F}_i + \begin{bmatrix} A_x & 0 & 0 \\ 0 & A_y & 0 \\ 0 & 0 & A_z \end{bmatrix} \begin{Bmatrix} \dot{x}_{des} \\ \dot{y}_{des} \\ \dot{z}_{des} \end{Bmatrix} + m \begin{Bmatrix} 0 \\ 0 \\ g \end{Bmatrix} + m \begin{Bmatrix} \ddot{x}_{des} \\ \ddot{y}_{des} \\ \ddot{z}_{des} \end{Bmatrix}. \tag{23}$$

Here, $\dot{x}_{des}, \dot{y}_{des}, \dot{z}_{des}$ and $\ddot{x}_{des}, \ddot{y}_{des}, \ddot{z}_{des}$ were taken to be the desired velocities and accelerations of the load. This is an approximation, assuming that the quadrotors are moving coherently with the load. Since the quadrotor can only produce thrust in the body frame z direction, the commanded thrust will be a projection of the desired force on the body frame z direction. Let us define the direction of the z body axis of the quadrotor as

$$z^e_{axis} = D^{q_i}_e \begin{Bmatrix} 0 \\ 0 \\ 1 \end{Bmatrix} \tag{24}$$

then

$$F_{cmd,i} = F^T_{des,i} z^e_{axis}. \tag{25}$$

The next step would be to calculate the moment commands as described in [7]. We will start by defining the desired direction of the z body axis as

$$z^e_{axis,des} = \frac{F_{des,i}}{\|F_{des,i}\|}. \tag{26}$$

Once obtaining the desired direction of the z body axis, we are left with one redundant degree of freedom (any direction of $y^e_{axis,des}$ that is orthogonal to $z^e_{axis,des}$ will be satisfying). We will close that degree of freedom by arbitrarily taking the projection of the vector

$$x^e_{arb,des} = \begin{Bmatrix} 1 \\ 0 \\ 0 \end{Bmatrix} \tag{27}$$

on the orthogonal plane to $z^e_{axis,des}$ (under the assumption that the chosen direction is not parallel to $z^e_{axis,des}$). Thus, we receive the desired rotation matrix

$$D^{q_i}_{e,des} = \begin{bmatrix} y^e_{axis,des} \times z^e_{axis,des} & y^e_{axis,des} & z^e_{axis,des} \end{bmatrix} \tag{28}$$

where

$$y^e_{axis,des} = \frac{z^e_{axis,des} \times x^e_{arb,des}}{\|z^e_{axis,des} \times x^e_{arb,des}\|}. \tag{29}$$

The relative attitude error will be defined as

$$e_R = \frac{1}{2} \left(D^e_{q_i,des} D^{q_i}_e - D^e_{q_i} D^{q_i}_{e,des} \right)^\vee \tag{30}$$

where $(\cdot)^\vee$ represents the "vee" map transformation from SE(3) to $\mathbb{R}^3$ (the inverse to the hat map). Note that the transformation is possible since the obtained matrix is skew-symmetric.

Now calculating the angular velocity error as

$$e_\Omega = \begin{Bmatrix} p \\ q \\ r \end{Bmatrix} - D^e_{q_i} D^{q_i}_{e,des} \begin{Bmatrix} p_d \\ q_d \\ r_d \end{Bmatrix} \tag{31}$$

where p_d, q_d, r_d are the desired angular rates calculated from

$$\begin{Bmatrix} p_d \\ q_d \\ r_d \end{Bmatrix} = \left(D^e_{q_i,des} \dot{D}^{q_i}_{e,des} \right)^\vee \tag{32}$$

e_Ω is actually the angular velocity of the rotation matrix $D^e_{q_i,des} D^{q_i}_e$ since

$$\frac{d}{dt} \left(D^e_{q_i,des} D^{q_i}_e \right) = \left(D^e_{q_i,des} D^{q_i}_e \right) \hat{e}_\Omega \tag{33}$$

as was shown in [7]. Next, we will consider the integral element of the attitude error with zero initial conditions and calculate the final commanded moments as

$$M_{cmd} = -K_R e_R - K_\Omega e_\Omega - K_{RI} e_{RI} + \begin{Bmatrix} p \\ q \\ r \end{Bmatrix} \times I_q \begin{Bmatrix} p \\ q \\ r \end{Bmatrix} \tag{34}$$

where $e_{RI} = \int_0^t e_R d\tau$ and the initial conditions were set to be zero. Including the integral term is a proposition made in [9] to improve the robustness of the controller against constant disturbances and was found useful when placing the link of each quadrotor at an offset from its c.g.. K_R,K_Ω and K_{RI} are positive constants. [7, 9] include stability proof for controllers similar to the one presented here. As discussed, a few adjustments were made along the development, hence, more work is needed to be done in order to prove stability of the developed controller and is not included in this work. Performance of the controller will be tested under different simulations as part of the whole control structure forward on.

4 Trajectory generation

In order to test the control structure for a varying trajectory, the following polynomial was constructed

$$s = \frac{6}{t_f^5} (s_f - s_0) t^5 - \frac{15}{t_f^4} (s_f - s_0) t^4 + \frac{10}{t_f^3} (s_f - s_0) t^3 + s_0 \tag{35}$$

which provides a smooth trajectory that takes us from an initial state s_0 to a final state s_f in a given desired transportation time t_f. Such trajectory was calculated for each state independently. If required, it is quite straight forward to find the derivatives of a desired state produced using the above polynomial.

5 Simulation

Using the model developed in the previous sections, a simulation of a three quadrotors configuration connected to a load was modeled. This section will provide simulation results for different scenarios to test the robustness and performance of the constructed control structure. The simulation parameters are given in Table 3. Each simulation started from a hovering initial conditions calculated from an initial run of the optimization problem, where all the initial states of the load are zero besides the height which is set to be $1\,(m)$:

$$\begin{Bmatrix} x & y & z & \phi & \theta & \psi & V_x & V_y & V_z & p & q & r \end{Bmatrix}^T = \begin{Bmatrix} 0 & 0 & 1\,(m) & 0 & 0 & 0 & 0 & 0 & 0 & 0 & 0 & 0 \end{Bmatrix}^T.$$

The safety distance between every two quadrotors was chosen to be 1 m plus twice the rotor arm length. We expect that constraint to be slightly violated during a maneuver until reaching steady state. For most of the simulations the cables were connected at the c.g. of each quadrotor. One simulation

where that is not the case will be displayed. The optimization problem is solved every given time step and the calculated value is kept constant until the next iteration. The geometric controller gains and LQR weights are given in Table 4. The corresponding calculated LQR gains are:

$$K_{LQR} = \begin{bmatrix} 0.5 & 0 & 0 & 0 & 0 & 0 & 1.0071 & 0 & 0 & 0 & 0 & 0 \\ 0 & 0.5 & 0 & 0 & 0 & 0 & 0 & 1.0071 & 0 & 0 & 0 & 0 \\ 0 & 0 & 0.5 & 0 & 0 & 0 & 0 & 0 & 1.0071 & 0 & 0 & 0 \\ 0 & 0 & 0 & 0.8 & 0 & 0 & 0 & 0 & 0 & 0.0955 & 0 & 0 \\ 0 & 0 & 0 & 0 & 0.8 & 0 & 0 & 0 & 0 & 0 & 0.0955 & 0 \\ 0 & 0 & 0 & 0 & 0 & 0.8 & 0 & 0 & 0 & 0 & 0 & 0.0955 \end{bmatrix} \tag{36}$$

Table 3: 3 quadrotors configuration simulation parameters

Parameter	Value	Units	Interpretation
ρ_1	$\{0.4 \quad 0.2 \quad 0.1\}^T$	m	load attachment points (relative to the load c.g.)
ρ_2	$\{0.4 \quad -0.2 \quad 0.1\}^T$	m	load attachment points (relative to the load c.g.)
ρ_3	$\{-0.4 \quad 0 \quad 0.1\}^T$	m	load attachment points (relative to the load c.g.)
R_{q1}	$\{0 \quad 0 \quad 0\}^T$	m	attachment point on quadrotor (relative to the quadrotor c.g.)
R_{q2}	$\{0 \quad 0 \quad 0\}^T$	m	attachment point on quadrotor (relative to the quadrotor c.g.)
R_{q3}	$\{0 \quad 0 \quad 0\}^T$	m	attachment point on quadrotor (relative to the quadrotor c.g.)
d_s	1.45	m	safety distance between every set of two quadrotors
T_{opt}	0.05	sec	Optimization problem step time

Table 4: Controllers gains

Parameter	Value	Interpretation
Q_{LQR}	$diag\begin{bmatrix}100 & 100 & 100 & 400 & 400 & 400 & 4 & 4 & 4 & 4 & 4 & 4\end{bmatrix}$	LQR states weights
R_{LQR}	$diag\begin{bmatrix}400 & 400 & 400 & 625 & 625 & 625\end{bmatrix}$	LQR control weights (first three relate to forces, latter three relate to moments)
N_{LQR}	$0 \in \mathbb{R}^{12\times 6}$	LQR coupling matrix weights
K_R	1.1	Geometric controller attitude error gain
K_Ω	0.2	Geometric controller angular rate error gain
K_{RI}	0.5	Geometric controller attitude error integrator gain
K_{pI}	0.075	Augmented integrated position error gains

5.1 Position and attitude maneuver

We will start off by showing a simple, no disturbance, cables connected at the quadrotors c.g. maneuver. The maneuver begins in the prescribed initial states

$$\{x \quad y \quad z \quad \phi \quad \theta \quad \psi \quad V_x \quad V_y \quad V_z \quad p \quad q \quad r\}^T = \{0 \quad 0 \quad 1\,(m) \quad 0 \quad 0 \quad 0 \quad 0 \quad 0 \quad 0 \quad 0 \quad 0 \quad 0\}^T$$

and ends in

$$\begin{Bmatrix} x \\ y \\ z \\ \phi \\ \theta \\ \psi \\ V_x \\ V_y \\ V_z \\ p \\ q \\ r \end{Bmatrix} = \begin{Bmatrix} 5\,(m) \\ 3\,(m) \\ 8\,(m) \\ 10^\circ \\ -10^\circ \\ 70^\circ \\ 0 \\ 0 \\ 0 \\ 0 \\ 0 \\ 0 \end{Bmatrix},$$

the desired transportation time is set to be 20 seconds (after that time, the load is commanded to maintain steady state). The trajectory is generated as described in section 4. The results are shown in Figs. 2 to 5. As can be seen in Fig. 3, in terms of position and attitude, the tracking errors are quite small and decay to zero after about 40 seconds. In Fig. 4 on the top graph we see that the acceleration of the load remains smooth and moderate, no sudden impulses, however it does vibrate slowly until completely decaying. On the middle graph we see that the rear quadrotor carries more weight than the two front quadrotors. It makes sense considering the attachment points on the load. On the bottom graph we see that the quadrotor separation constraints were kept during the maneuver except for a few minor violations - less than 1% violation from the desired value. Those were taken under consideration when choosing the required separation distances. Once reaching steady state, the constraints are maintained and settle on a value close the the minimal bound.

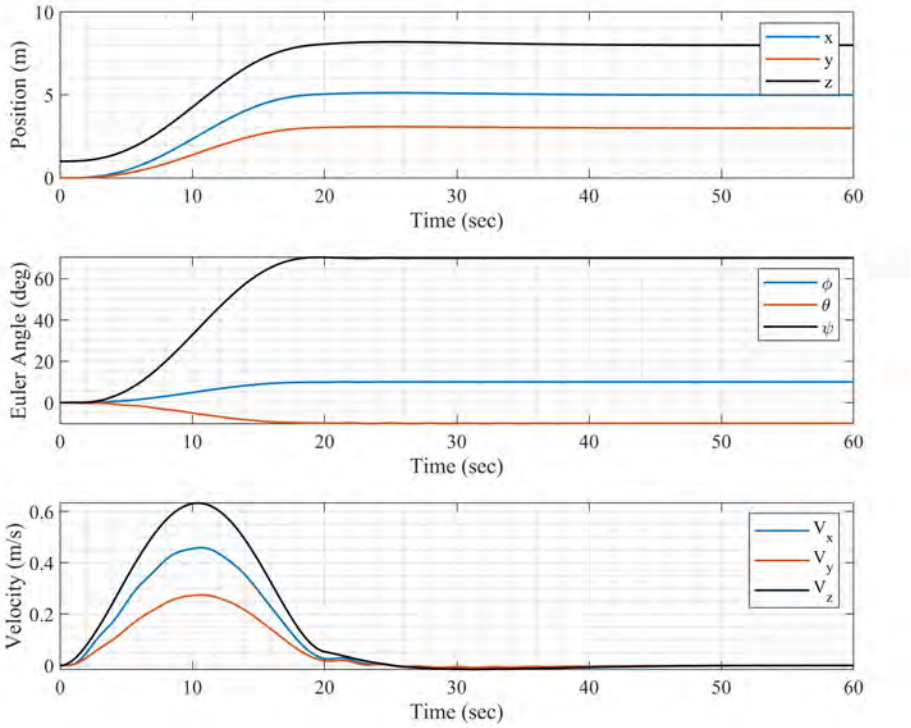

Figure 2: Payload position, attitude and velocity, no disturbances simulation

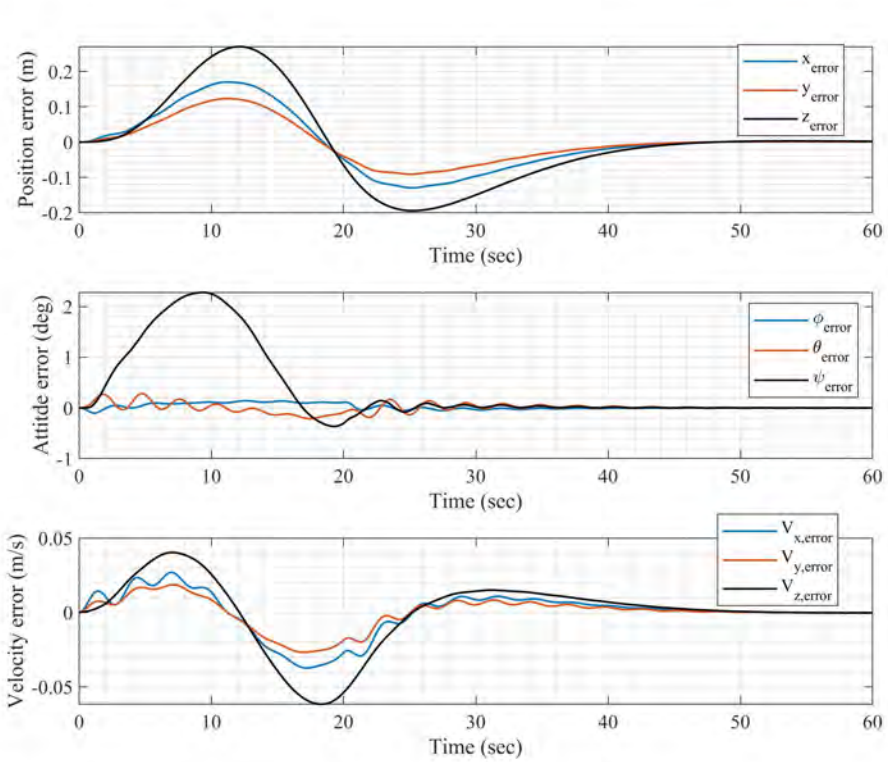

Figure 3: Payload position, attitude and velocity errors, no disturbances simulation

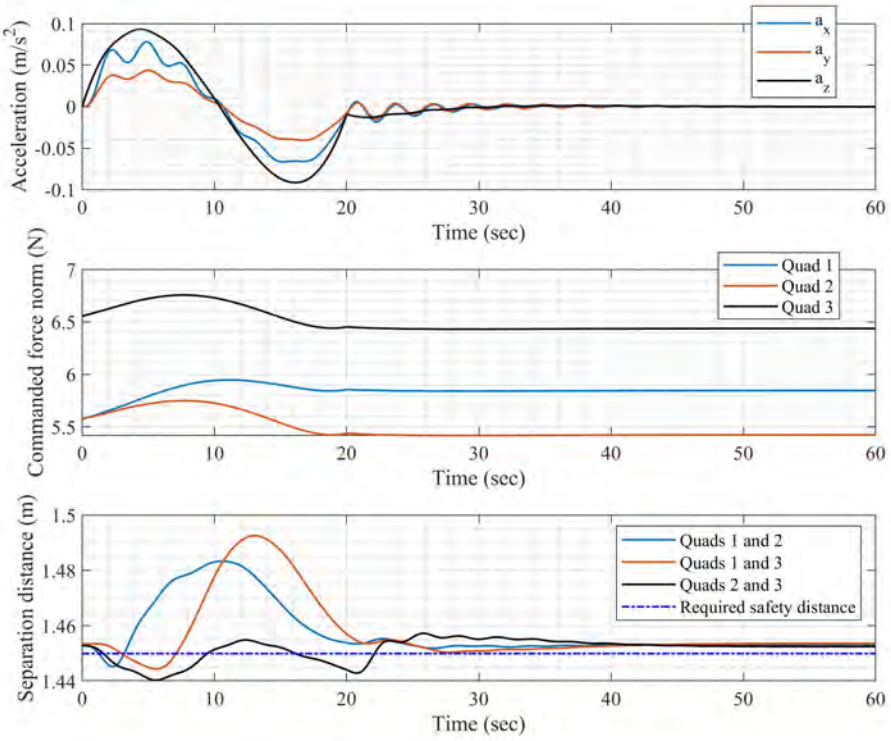

Figure 4: Acceleration, forces commands and separation constraints, no disturbances simulation

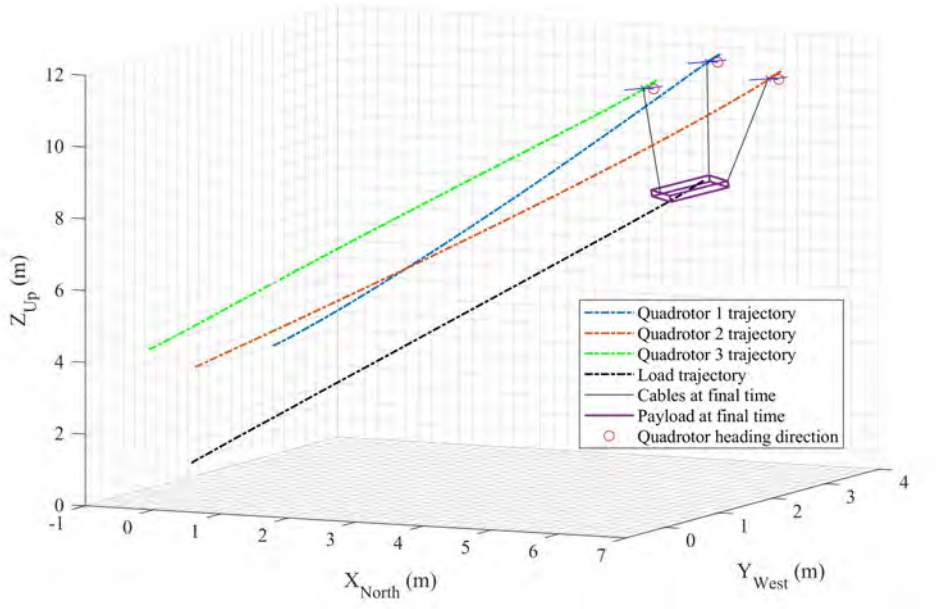

Figure 5: 3D trajectory, no disturbances simulation

5.2 Position and attitude maneuver, cables attachment points are not at the quadrotors c.g.

Here we analyze the simulation results for a maneuver identical to the one described in the previous case, while the attachment point on the quadrotors was shifted from their respected c.g.'s. In particular, the attachment points were set to be

$$R_{q1} = \begin{Bmatrix} 0.05 & 0.04 & -0.02 \end{Bmatrix}^T, R_{q2} = \begin{Bmatrix} -0.02 & -0.05 & -0.05 \end{Bmatrix}^T, R_{q3} = \begin{Bmatrix} -0.04 & 0.05 & -0.04 \end{Bmatrix}^T. \tag{37}$$

The values were chosen arbitrarily in a way they will challenge the control system but still be feasible and are given in meters. The desired transportation time is again 20 seconds. The results are shown in Figs. 6 to 9. As can be seen in Fig. 7, in terms of position the tracking errors are inferior to the previous case, but still satisfactory. In this case, the attitude errors are the most significant, although they still decay after the transient, and are very small at the end of the maneuver. In Fig. 8 on the top graph we see that the acceleration of the load is higher than in the previous simulation. On the bottom graph we see that the violation of the minimal separation distance is much more significant than on the previous simulation and reaches around 25% violation. This is something that should be taken under consideration when choosing the separation distance and assessing the attachment points errors on the quadrotors. Once reaching steady state, the constraints are maintained and settle on a value close the the minimal bound. As expected, the system behavior is inferior to the one in the previous section, however, the results are still satisfying.

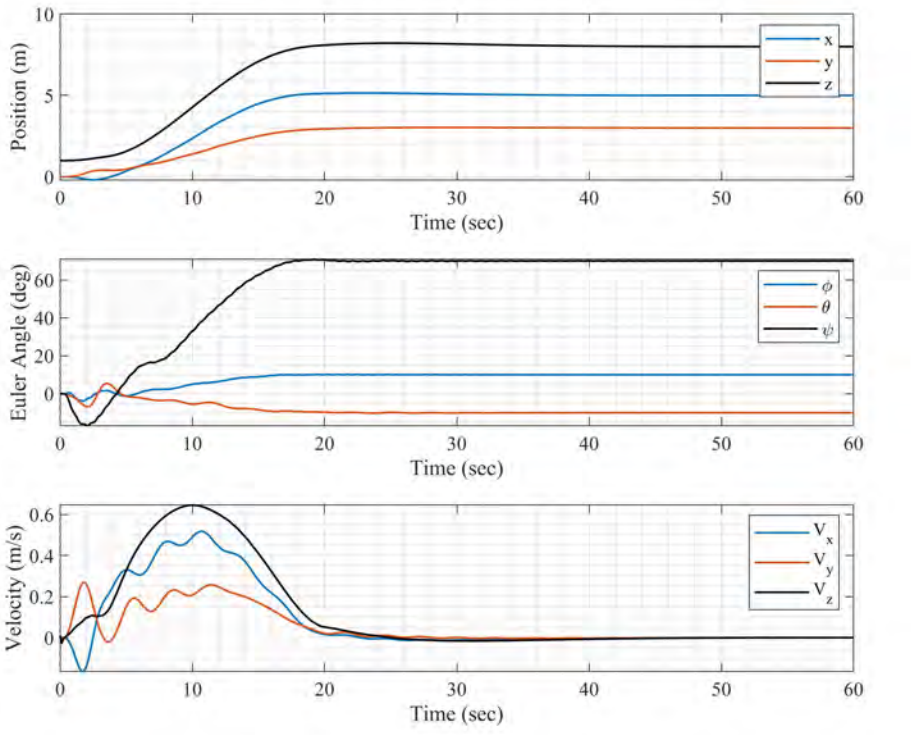

Figure 6: Payload position, attitude and velocity, offset attachment simulation

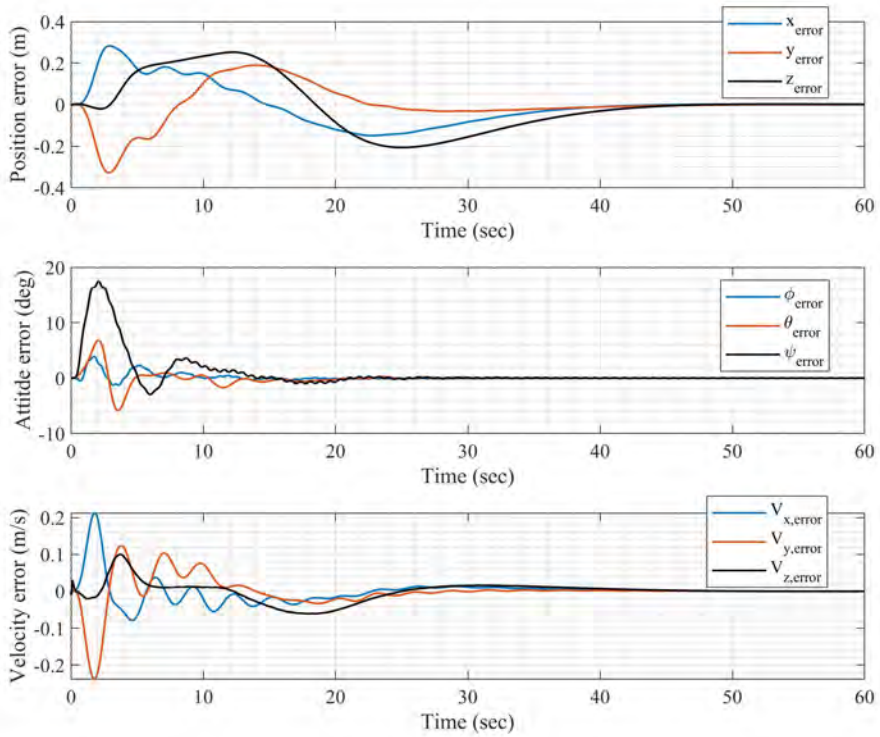

Figure 7: Payload position, attitude and velocity errors, offset attachment simulation

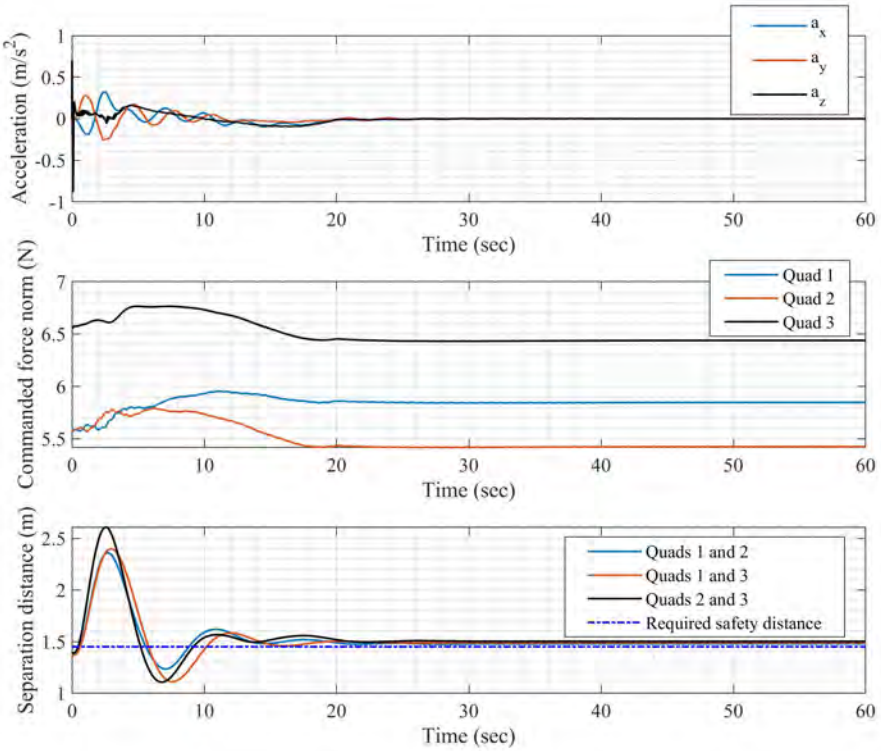

Figure 8: Acceleration, forces commands and separation constraints, offset attachment simulation

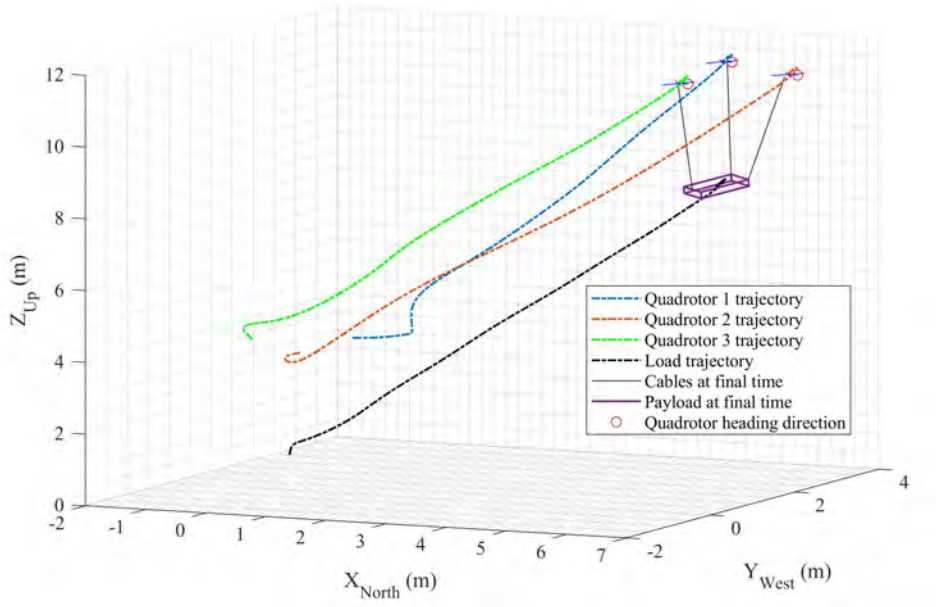

Figure 9: 3D trajectory, offset attachment simulation

5.3 Constant velocity maneuver with constant disturbance

For this simulation, we start from the rest hovering initial conditions again. At time $t = 1\,(sec)$, a command to accelerate in the x direction from $0\,\left(\frac{m}{s}\right)$ to $2\,\left(\frac{m}{s}\right)$ in 6 seconds is applied using the trajectory generation polynomial. At time $t = 35\,(sec)$, a step of the size $2\,(N)$ in the y direction and $-1\,(N)$ in the z direction is activated as a constant disturbance on the load. The disturbance is smoothed using the second order transfer function

$$H_f\,(s) = \frac{225}{s^2 + 21s + 225}. \tag{38}$$

The results are shown in Figs. 10 to 13. As can be seen in Fig. 11, at the beginning of the movement, in the acceleration phase, a position error in the acceleration direction is increasing. However, once settling on a certain speed, the controllers compensate for the error and eventually after a small amount of time reaches the desired states. It is also possible to see in the middle graph that the acceleration causes a vibrating error around θ that decays over time. Once the disturbance is activated, we can see it causes errors in all states that again decay over time. In Fig. 12 on the middle graph we see that once the disturbance is activated, the required forces changes accordingly to compensate and reach the new steady state. On the bottom graph we see that before the disturbance is activated, the violations of the separation distances are again minor and maintained under 5%. The disturbance causes a violation that reaches around 10% and decays over time.

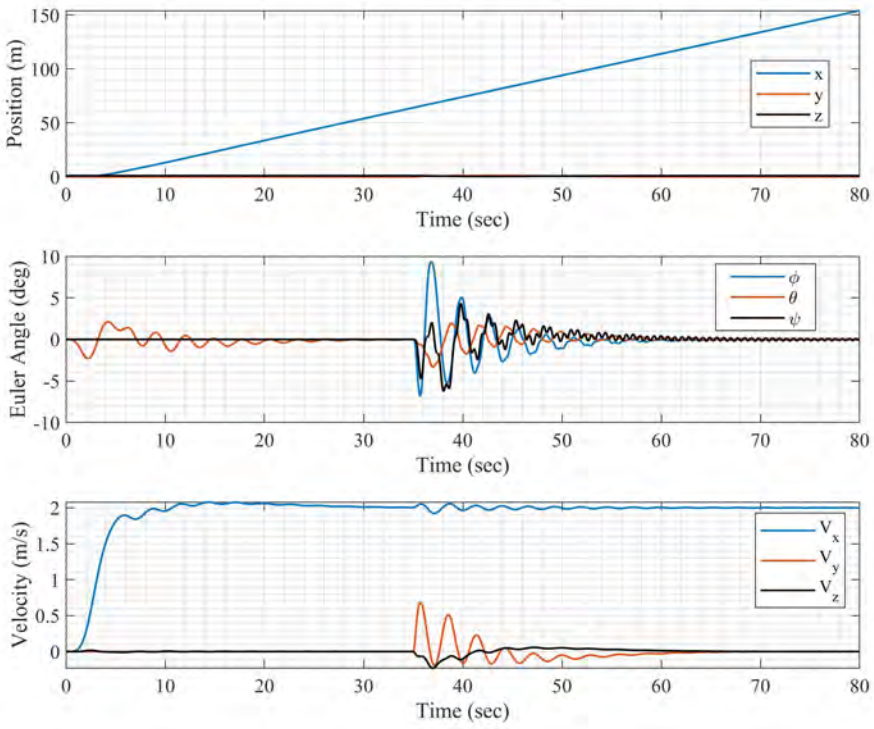

Figure 10: Payload position, attitude and velocity, constant velocity simulation

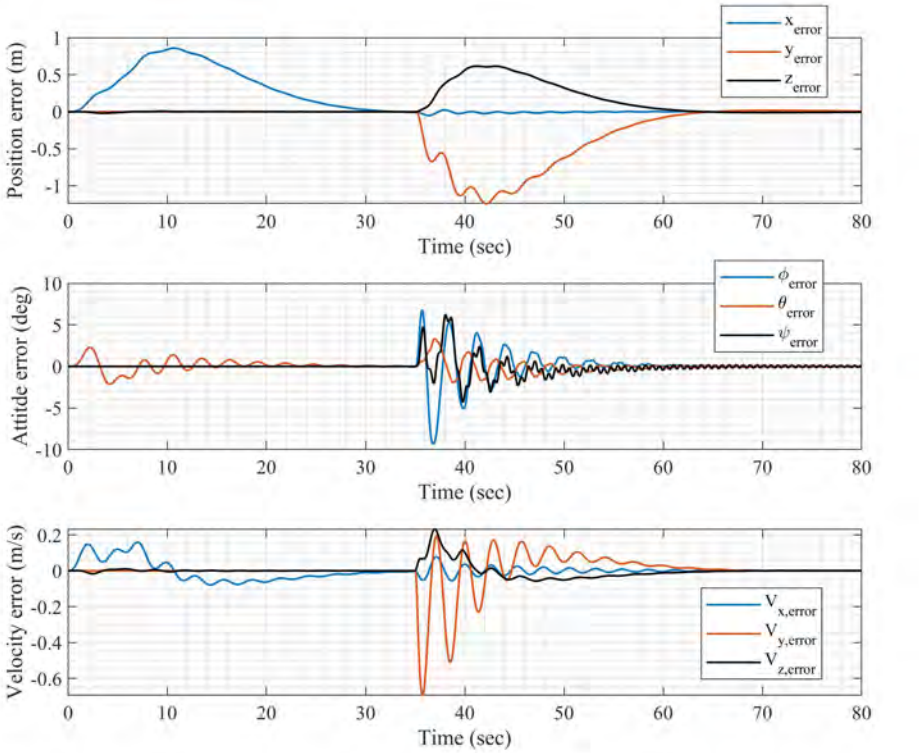

Figure 11: Payload position, attitude and velocity errors, constant velocity simulation

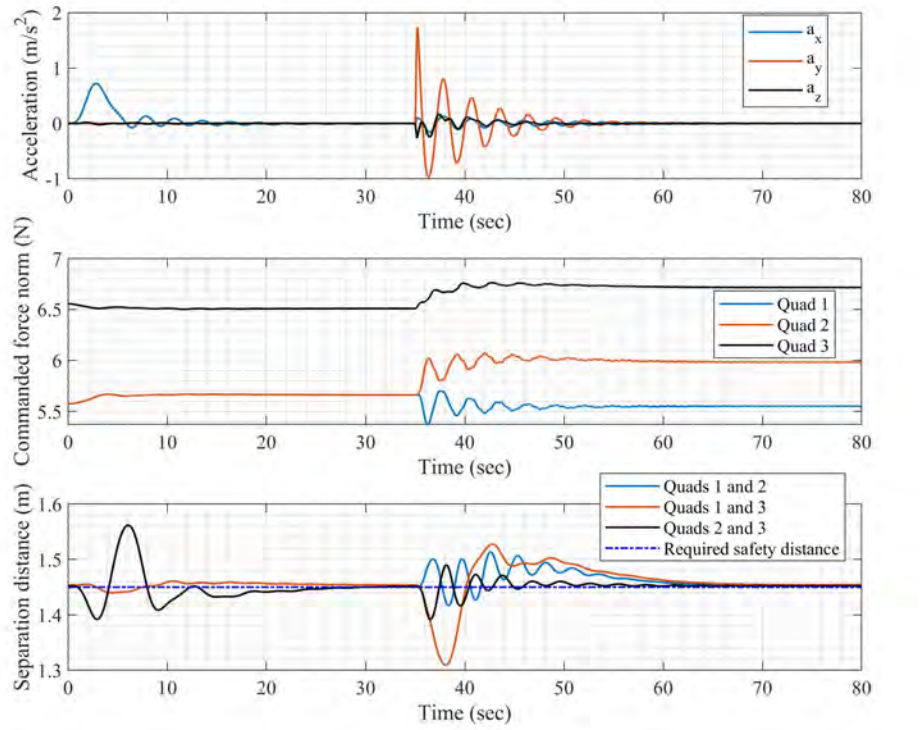

Figure 12: Acceleration, forces commands and separation constraints, constant velocity simulation

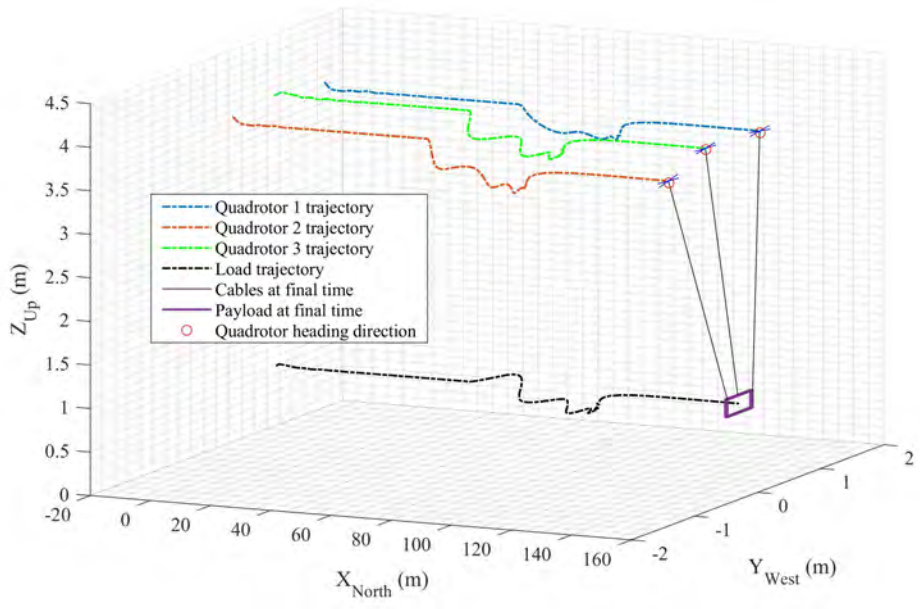

Figure 13: 3D trajectory, constant velocity simulation. Note that the payload dimensions looks smeared because of the axis scales, however, the dimensions are the same as in previous simulations

5.4 Simulation results discussion

After testing our controllers under varying conditions and disturbances we conclude that our system provides satisfying results and is robust to constant disturbances. A few remarks should be made:

- When considering attachment points which are not at the c.g. of the quadrotors, we should expect violations in separation distances constraints between the quadrotors and take safety interval. In our examined cases at no simulation we reached below a separation distance of 1 (m) which is more than twice the distance to collision, and hence we are satisfied with that result.
- Further work could be done to try and improve the transient performance when it comes to attitude behavior of the load. During the work, faster and less vibrating (in attitude perspective) controllers were designed, however, those were not robust against disturbances and parameter inaccuracies. Therefore, the prescribed slower and more vibrating controller was chosen considering we want the system to be robust against different disturbances.
- The forces that was required from each quadrotor were at all times lower than the maximum force allowed. The cables remained taut at all times.
- Attitude control is limited to around 30° for ϕ or θ, and around 20° for both at the same time. ψ is not limited. For higher values the optimization problem for our configuration considering the constraints reaches the point where it can no longer find a feasible solution and the system loses stability. This is also something to be aware of when considering different disturbances that might drive the attitude of the load beyond those values. If one wishes to reach more extreme attitude states, it is possible to consider different attachment configuration, or to loosen the optimization constraints.

6 Conclusion

As shown in this project, the problem of controlling the multi agent system is not an easy task. It is a highly complex nonlinear MIMO system and a lot of constraints and conditions must be met. During this project we covered the following subjects:

- We constructed a simulation environment for the n quadrotors connected to a load system.
- An LQR controller that calculates required forces and moments such that the load will follow desired trajectory was designed.
- We defined an optimization problem that divide the burden of the load between the available quadrotors while maintaining certain constraints.
- We designed a geometric controller for the quadrotors such that each quadrotor will provide the required force.
- The simulation was tested under three different scenarios with and without disturbances, the results were analyzed and discussed.

In the literature, there has been quite a few control methods that were applied to similar problems. In [3] a geometric controller was designed to make sure the load carried by a flock of quadrotors follows a certain trajectory. In [4] a LQR-PID method was used in order to achieve stability of a similar system while maintaining a certain formation of the flock and following a given trajectory. In [2] a Sliding Mode Control (SMC) method was implemented to ensure stability of a similar system. The control structure designed in this work was inspired from the ideas presented in the above articles. The resulted controller was found to provide good tracking and disturbance rejection abilities. This work provides the infrastructure for further research in the field of terrain following. In future work we will address the problem of incorporating the terrain following ability on a slung load carried by multi-UAV system such as the one presented in this work.

Acknowledgements

I would like to thank Prof. Moshe Idan for the dedicated mentoring of this project, and to Mr. Dudu Marcovitz for enriching and aiding with this work.

References

[1] Zu Qun Li, Joseph F. Horny, and Jack W. Langelaanz. Coordinated transport of a slung load by a team of autonomous rotorcraft. *AIAA Guidance, Navigation, and Control Conference*, (January), 2014.

[2] Hyun Shik Oh, Min Jea Tahk, Dong Wan Yoo, and Byung Yoon Lee. Robust Stabilization Technique for the Leader Steering Slung-Load System/Using Sliding Mode Control. *International Journal of Aeronautical and Space Sciences*, 19(4):932–944, 2018.

[3] Taeyoung Lee. Geometric Control of Quadrotor UAVs Transporting a Cable-Suspended Rigid Body. *IEEE Transactions on Control Systems Technology*, 26(1):255–264, jan 2018.

[4] Behzad Shirani, Majdeddin Najafi, and Iman Izadi. Cooperative load transportation using multiple UAVs. *Aerospace Science and Technology*, 84:158–169, 2019.

[5] Teppo Luukkonen. Modeling and control of quadcopter. *Independent research project in applied mathematics, Espoo*, 22, 2011.

[6] Patricio Cruz and Rafael Fierro. Autonomous lift of a cable-suspended load by an unmanned aerial robot. *2014 IEEE Conference on Control Applications, CCA 2014*, pages 802–807, 2014.

[7] Taeyoung Lee, Melvin Leok, and N. Harris McClamroch. Control of Complex Maneuvers for a Quadrotor UAV using Geometric Methods on SE(3). (3), 2010.

[8] Junyi Geng and Jack W. Langelaan. Implementation and demonstration of coordinated transport of a slung load by a team of rotorcraft. *AIAA Scitech 2019 Forum*, (January):1–19, 2019.

[9] Farhad A. Goodarzi and Taeyoung Lee. Stabilization of a Rigid Body Payload with Multiple Cooperative Quadrotors. *Journal of Dynamic Systems, Measurement and Control, Transactions of the ASME*, 138(12):1–17, 2016.